International Conference on Space Optics—ICSO 2012

Ajaccio, Corse

9–12 October 2012

Edited by Bruno Cugny, Errico Armandillo, and Nikos Karafolas

Characterization of an ultra-stable optical cavity developed in the industry for space applications

Berengere Argence

S. Bize

P. Lemonde

G. Santarelli

et al.

esa icso proceedings cnes

International Conference on Space Optics — ICSO 2012, edited by Bruno Cugny, Errico Armandillo, Nikos Karafolas
Proc. of SPIE Vol. 10564, 105641O · © 2012 ESA and CNES · CCC code: 0277-786X/17/$18 · doi: 10.1117/12.2309037

Characterization of an ultra-stable optical cavity developed in the industry for space applications.

B. Argence, S. Bize, P. Lemonde and G. Santarelli
LNE-SYRTE
Observatoire de Paris, CNRS, UPMC
Paris, France
Berengere.Argence@obspm.fr

E. Prevost and R. Le Goff
SODERN
20 Av. Descartes
Limeil-Brevannes, France

T. Lévèque
CNES, Centre National d'Etudes Spatiales
18 Av. Edouard Belin
Toulouse, France

***Abstract*— We report the main characteristics and performances of the first – to our knowledge – prototype of an ultra-stable cavity designed and produced by industry with the aim of space missions. The cavity is a 100 mm long cylinder rigidly held at its midplane by an engineered mechanical interface providing an efficient decoupling from thermal and vibration perturbations. The spacer is made from Ultra-Low Expansion (ULE) glass and mirrors substrate from fused silica to reduce the thermal noise limit to $4x10^{-16}$. Finite element modeling was performed in order to minimize thermal and vibration sensitivities while getting a high fundamental resonance frequency. The system was designed to be transportable, acceleration tolerant (up to several g) and temperature range compliant [-33°C; +73°C]. The axial vibration sensitivity was evaluated at $4x10^{-11}$ /(ms^{-2}), while the transverse one is < $1x10^{-11}$ /(ms^{-2}). The fractional frequency instability is < $1x10^{-15}$ from 0.1 to few seconds and reaches 5-$6x10^{-16}$ at 1s.**

I. Introduction

Frequency-stable lasers are important tools whose present applications include modern frequency metrology [1-4], gravitational wave detection [5], fundamental physics tests [6,7], coherent optical links [8] and related space applications [9]. Frequency stability can be achieved by locking the laser to a rigid Fabry-Perot (FP) cavity. The ultimate fundamental limit of this system is the thermal noise (Brownian motion). Nevertheless, to reach this limit, different sources of noise have to be drastically reduced. Among them, the most important ones are thermal and vibration perturbations. During the last decade, strong efforts have been done in this way to isolate cavities and make them insensitive by design to environmental perturbations. However, most of these cavities have been designed in a laboratory view and making them compatible with transport and space requirements involves a major redesign of the cavity and its assembly. Recently, significant progress towards cavity designs with low vibration sensitivity [10], transportability [11] and robustness [12] has been achieved.

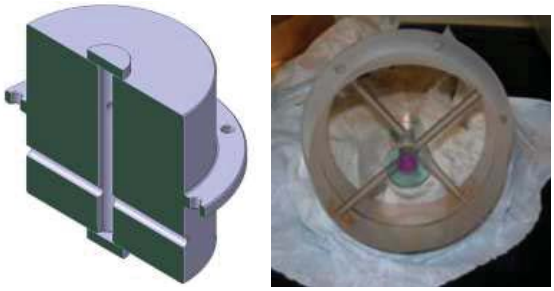

Figure 1. Drawing (left) and photography (right) of the cavity

This work reports on the design and the characterization of an ultra-stable cavity developed by space industry. The main idea is to capitalize on the space instrument development know-how to accommodate for constraints not usual in laboratory environment. The system was designed to support acceleration up to several g and temperature variation range of [-33°C; 73°C] during transport and storage, while keeping good frequency stability performances. Extensive thermo-mechanical modeling was performed to obtain low thermal and vibration sensitivities.

II. Finite Element Modeling

A. Cavity design and geometry

The cavity has a cylindrical geometry of length 100 mm and diameter 110 mm (see Fig. 1). The reflection coating of the mirrors allows operation at 1.542µm, in the telecom wavelength region. The free spectral range is 1.5 GHz.

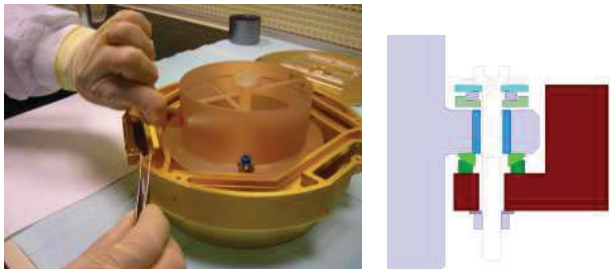

Figure 2. (Left) Photography of the cavity and its CFD, see text for details. (Right) Drawing of the setup used to fix the cavity to the CFD.

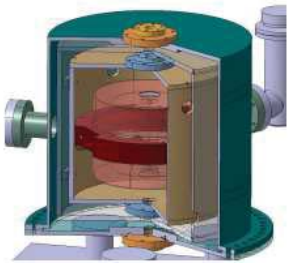

Figure 3. Drawing of the system including cavity, interface, shields and vacuum chamber.

The mirror configuration is plano-concave (radius of curvature of 500mm). The spacer is made from Ultra-Low Expansion (ULE) glass, with Fused Silica (FS) mirrors substrates in order to reduce thermal noise floor [13,14]. For the present geometry, the calculated flicker thermal noise is ~ $4x10^{-16}$, dominated by the coatings. This is a factor > 2 better than an all-ULE cavity. The main drawback is an increase of the thermal sensitivity – coefficient of thermal expansion (CTE) – to about ~ 10^{-7}/K, a value that we verified experimentally.

A ring in the midplane of the cylinder allows rigidly attaching the cavity (see Fig. 1). The cavity body is machined from a monolithic block of ULE. The ring has a diameter of 140mm and a thickness of 7mm. Six holes distributed equidistantly were drilled, corresponding to two sets of three holes possible to bind the cavity. The choice of the set was done considering the parallelism of the surfaces of the ring at the positions of the holes. The cavity is then held symmetrically in three points separated by 120 degrees by a mechanical interface, see paragraph C. The shape of the central ring (thickness and diameter) was optimized to minimize deformations of the cavity. The diameter of the spacer was designed to minimize the transverse vibration sensitivities and the position of the vents holes was determined to maintain stiffness.

B. Thermal Shields

The cavity is protected against thermal perturbations by three gold coated aluminum shields inside a stainless steel vacuum chamber, see Fig. 3 where the most internal shield is not depicted. Aluminum provides low temperature gradient while maintaining good mechanical stiffness. To keep the first mechanical resonance as high as possible and to be compatible with the requirements of transport, each shield is rigidly fixed to the upstream one. This passive thermal shielding was designed to act as a 2^{nd} / 3^{rd} order low pass filter with the larger time constant of ~ 2.5 days. The vacuum chamber is a cylinder of a radius of 170 mm and a height of 300 mm. The total mass of the cavity assembly (40 kg) is dominated by the mass of this external vacuum enclosure (~20kg). The use of titanium for future versions is preferable since for similar thermo-mechanical properties, the density of this material is 40% lower. A 2 liter/second ion pump ensures a vacuum level $<10^{-6}$ mbar. A residual gas analysis revealed that the molecular hydrogen H_2 from the stainless steel can limit the vacuum level, this could be solved by using titanium instead of stainless steel.

C. Mechanical Interface

A critical part of the system is the interface between this cavity and the internal shield. The interface is designed to decouple both mechanically and thermally the cavity. In addition, the interface needs to preserve the properties of the cavity design in term of mechanical symmetry. The overall task is complicated by the significant mass of the cavity of about 2.2kg. Much efforts have been devoted to modelizing this part called CFD (Cavity Fastening Device), represented in Fig. 2. This interface is made of Invar, chosen to reduce the differential temperature expansions and consequently constraints and deformations applied to the cavity.

A dual cantilever system rigidly links the CFD to the cavity and the inner thermal shield. Studies have been performed to optimize their geometry and their flexibility. These cantilevers can thus filter the constraints and deformations due to temperature variations or vibrations while maintaining a high degree of stiffness so that the fundamental eigen mode is sufficiently high. The first mechanical resonance of the whole system - excluding the holding posts - was designed to be ~300Hz, quite high considering the mass of the system (40 kg). To avoid any permanent moment of force and to prevent any break of ULE glass, studies were conducted to optimize the interface between the glass and the internal cantilevers. The cavity and the CFD are bolted with an optimized stack of washers, see right drawing on Fig. 2.

III. EXPERIMENTAL TEST SETUP

The experimental setup to lock a laser onto the cavity uses the Pound Drever Hall (PDH) method [15]. The scheme is presented in Fig 4. We use a low noise extended cavity diode laser (RIO Planex) with an output optical power of 15mW. A fibered voltage controlled Variable Optical Attenuator (VOA) is used to control the optical power sent into the cavity. A 10/90 splitter extracts 90% of the frequency stabilized beam. A polarizing beam splitter and a half waveplate allow fine tuning of the optical power. After passing through an optical isolator, the beam is

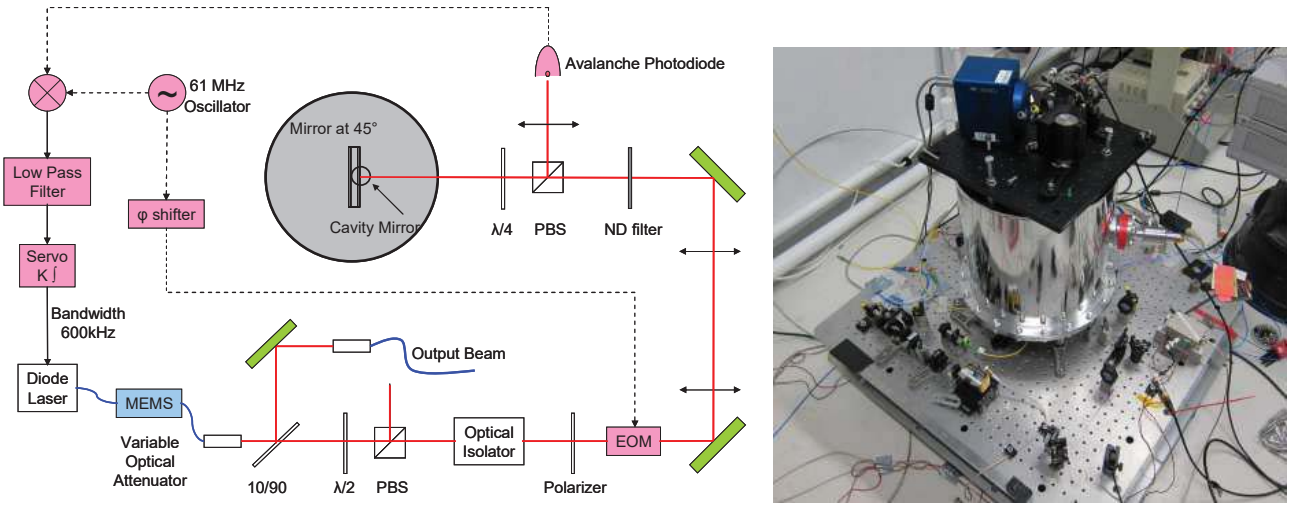

Figure 4. (Left) Experimental setup used to lock the diode laser onto the cavity following the PDH locking technique. Blue line: optical fiber path, Red line: free space path, Black line: electrical path
PBS: Polarizing Beam Splitter, λ/2(4): half (quarter) waveplate, EOM: Electro-Optical Modulator, ND: Neutral Density Filter
(Right) Photography of the experimental setup.

phase modulated at 61MHz using an Electro-Optical Modulator (EOM). We optimize the polarization before the EOM to minimize the residual amplitude modulation. We use two lenses to realize the mode-matching before injecting the beam into the cavity. The reflected beam is sensed with an avalanche photodiode. This detected signal is then mixed to a local oscillator to produce the error signal. The control loop only acts on the current of the diode with a bandwidth of 600 kHz. This setup is protected against environmental perturbations by a ~ 0.8 m^3 aluminum box with an acoustic absorber not shown in the photography of Fig. 4.

The linewidth of the cavity resonance FWHM is measured to be 3.9 ± 0.1 kHz, corresponding to a finesse of ~ 380 000.

We measure the optical power to frequency conversion coefficient to be about ~ 200 Hertz per µW transmitted. Consequently, to avoid frequency noise degradation due to optical power fluctuations, the injected power is actively controlled by the VOA. This system maintains a relative intensity noise (RIN) below -100 dB from 1 Hz to 1 kHz (bandwidth limited). This ensures that frequency fluctuations induced by optical power are lower than $1x10^{-16}$ at 1s.

IV. Characterization of the Cavity Assembly

A. Vibration sensitivity measurements

The cavity device was designed to minimize the effects of residual vibration in order to reduce frequency noise. The vibration measurement setup is presented in Fig 5. The cavity setup is shaken with either sinusoidal or chirped signals from 2 to 50 Hz using an active vibration isolation platform. The acceleration modulation is evaluated with a piezoelectric sensor.

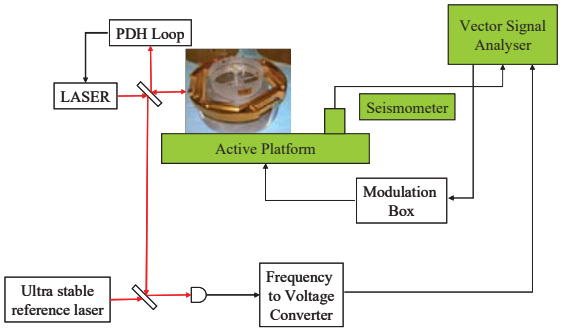

Figure 5. Vibration Sensitivity measurement setup.

The induced frequency modulation is measured using the beat-note between the diode laser locked to the cavity and another Ultra Stable reference Laser (USL). Frequency fluctuations are then converted with a homemade frequency-to-voltage converter. Both acceleration and frequency modulations are simultaneously obtained with a vector signal analyzer. The vibration sensitivity Γ*(f)* is then defined by the following equation:

$$\Gamma(f) = \frac{1}{\nu_0}\sqrt{\frac{S_\nu(f)}{S_a(f)}} \qquad (1)$$

where $S_\nu(f)$ and $S_a(f)$ are respectively the frequency and acceleration power spectral densities and ν_0 is the optical frequency equal to 194 THz.

With this setup, we evaluate the vertical vibration sensitivity to be (4 ± 0.5) $x10^{-11}$ /(ms^{-2}). The horizontal sensitivity is more

difficult to evaluate due to a strong coupling between the three orthogonal axes of the platform when a horizontal excitation is applied. Nevertheless, by modulating at discrete frequencies where the cross-coupling is minimum, we can evaluate the horizontal vibration sensitivity to be $(6 \pm 3)\ x10^{-12}\ /(ms^{-2})$.

B. Thermal shielding factor evaluation

Passive thermal shielding is an efficient way to reduce the overall temperature sensitivity on short time scale. From FEM, we expect from it a low pass filter with a time constant of ~ 2.5 days. To check these predictions, we apply a short temperature perturbation of ~ 4 °C. We simultaneously record the frequency of the laser locked onto the cavity and the temperature. We find that the passive thermal shielding can be modeled by a second order low pass filter with a first time constant of ~ 1.3 days and a second one of 2.2 days. There is then a good agreement between simulated and experimental values. With this thermal shielding factor, an active temperature control with a flicker noise floor of 0.1mK (Allan deviation) up to 10s is then sufficient to obtain a fractional frequency stability $< 5 \times 10^{-16}$ at 10s.

C. Frequency noise and stability

The frequency noise and stability of the laser locked to the cavity are evaluated by comparison with a reference USL. This measurement shows a frequency noise of about $10^{-2}\ Hz^2/Hz$ from 10Hz to 1 kHz. The frequency stability of the beat-note is below 1×10^{-15} from 0.1 to few seconds (linear drift removed) and reaches 7×10^{-16} at 1s. By removing the contribution of the reference USL, we obtain a 1s-stability of about 5.5×10^{-16}, close to the expected thermal limit.

V. Conclusion and Prospects

We report the characterization of the first ultra-stable Fabry-Perot cavity totally developed by a space industry. The system was designed to be robust, transportable, and able to withstand acceleration up to several g and temperature variations of ± 53K. Extensive thermo-mechanical modeling was performed to reduce thermal and vibration sensitivities. The passive thermal shield acts as a second order low pass filter with the larger time constant of about 2.2 days, in good agreement with the modeling. The measured axial vibration sensitivity is about $\sim 4 \times 10^{-11}\ /(m.s^{-2})$, while that in the transverse direction is about $\sim 6 \times 10^{-12}\ /(m.s^{-2})$. Although the axial coefficient is larger that expected from the design, these values of acceleration sensitivity would be sufficient in a satellite environment with acceleration below $10^{-5}\ m.s^{-2}$. A laser diode locked onto the cavity shows fractional frequency stability $< 10^{-15}$ from 0.1 to few seconds and $\sim 5 - 6 \times 10^{-16}$ at 1s.

A similar device is under development for the interrogation laser of a Strontium lattice clock (698nm), in the FP7/SOC2 European project framework. Regarding the good performances of this first prototype, minor modifications of the design can lead to a significant reduction of the overall mass and the thermal sensitivity (optimization of titanium enclosure and implementation of ULE compensation ring on mirror substrates). Additionally, for applications with lower frequency stability requirements, the use of a shorter cavity (50/70 mm) will lead to a strong improvement of the main critical parameters for space applications (mass, volume, resonance frequency and acceleration tolerance).

Acknowledgment

Authors thank W. Zhang, Z. Xu and Y. Le Coq for their contribution to the frequency stability measurements and J. Pinto and M. Lours for their assistance with electronics.

References

[1] H. Katori, “Optical lattice clocks and quantum metrology”, Nature Photon., vol. 5, pp. 203, 2011

[2] M. D. Swallows, M. Bishof, Y. Lin, S. Blatt, M. J. Martin, A. M. Rey and J. Ye “Suppression of Collisional Shifts in a Strongly Interacting Lattice Clock”, Science, vol. 331, pp. 1043, 2011.

[3] N. Huntemann, M. Okhapkin, B. Lipphardt, S. Weyers, Chr. Tamm and E. Peik, “High-Accuracy Optical Clock Based on the Octupole Transition in 171Yb+”, Phys. Rev. Lett., vol. 108, pp. 090801, 2012.

[4] J.A. Sherman, N.D. Lemke, N. Hinkley, M. Pizzocaro, R.W. Fox, A.D. Ludlow and C.W. Oates “High-Accuracy Measurement of Atomic Polarizability in an Optical Lattice Clock”, Phys. Rev. Lett., vol. 108, pp. 153002-5, 2012.

[5] F. Acernese et al., “Virgo status”, Class. Quantum Grav., vol 25, pp. 184001, 2008.

[6] S. Herrmann, A. Senger, K. Mohle, M. Nagel, E.V. Kovalchuk and A. Peters, "Rotating optical cavity experiment testing Lorentz invariance at the 10^{-17} level", Phys. Rev. D, vol. 80, pp. 105011, 2009.

[7] C. W. Chou, D. B. Hume, T. Rosenband and D. J. Wineland, “Optical Clocks and Relativity”, Science, vol. 329, pp. 1630 – 1633, 2010.

[8] H. Jiang et al., “Long-Distance frequency transfer over an urban fiber link using optical phase stabilization”, J. Opt. Soc. Am. B, vol. 25, issue 12, pp. 2029, 2008.

[9] K. Danzmann and A. Rüdiger, “LISA technology – concept, status, prospects”, Class. Quantum Grav., vol 20, S1, 2003.

[10] S. Webster and P. Gill, “Force-insensitive optical cavity”, Opt. Lett., vol. 36, pp. 3572-3574, 2011.

[11] S. Vogt, C. Lisdat, T. Legero, U. Sterr, I. Ernsting, A. Nevsky and S. Schiller, “Demonstration of a Transportable 1 Hz-Linewidth Laser,” Appl. Phys. B, vol. 104, pp. 741-745, 2011.

[12] D. R. Leibrandt, M. J. Thorpe, J. C. Bergquist, and T. Rosenband, “Field-test of a robust, portable, frequency-stable laser,” Opt. Express, vol. 19, pp. 10278-10286, 2011.

[13] J. Millo et al., “Ultrastable lasers based on vibration insensitive cavities”, Phys. Rev. A, vol. 79, pp. 053829, 2009.

[14] K. Numata, A. Kemery and J. Camp, “Thermal-Noise Limit in the Frequency Stabilization of Lasers with Rigid Cavities”, Phys. Rev Lett., vol. 93, pp. 250602, 2004.

[15] R. W. Drever et al., “Laser phase and frequency stabilization using an optical resonator”, Appl. Phys. B: Lasers Opt., vol. 31, pp. 97, 1983.